RESEARCH REPORT

VTT-R-00469-24

Spent nuclear fuel inventory calculations with a micro-depletion model

Authors: Topias Kähkönen

Confidentiality: VTT Public

VTT

beyond the obvious

Report's title	
Spent nuclear fuel inventory calculations with a micro-depletion model	
Customer, contact person, address	**Order reference**
Valtion ydinjätehuoltorahasto	SAFER 2028
Project name	**Project number/Short name**
NOTCO 2024 / SAFER 2028	371307/NOTCO
Author(s)	**Pages**
Topias Kähkönen	16/–
Keywords	**Report identification code**
Micro depletion, Inventory calculations, Homogenization, Ants, Serpent	VTT-R-00469-24

Summary
Advanced nodal methods track concentrations of neutronically significant nuclides with micro depletion to improve the accuracy of reactor simulations. Despite micro depletion successfully calculates the transmutation of nuclides using homogenized microscopic cross sections, the application for spent nuclear fuel inventory calculations is understudied. This study aims to create a micro-depletion model for homogeneous reactor geometry equivalent to the heterogeneous depletion solver in Serpent. The work compares a micro-depletion-based PWR fuel inventory to a high-fidelity Monte Carlo solution. The objective is to develop a fuel-depletion model for nodal code Ants enabling the evaluation of essential fuel properties for full-core reactor simulations and back-end fuel cycle studies.

Confidentiality	VTT Public

Espoo 21.8.2024

Written by	**Reviewed by**
Topias Kähkönen, Research Scientist	Antti Rintala, Research Scientist

VTT's contact address
VTT Technical Research Centre of Finland Ltd, P.O. Box 1000, FI-02044 VTT, FINLAND

Distribution (customer and VTT)
SAFER 2028

Approval

VTT TECHNICAL RESEARCH CENTRE OF FINLAND LTD

Date:	30.8.2024
Signature:	Häkkinen Silja 912690884 Digitally signed by Häkkinen Silja 912690884 Date: 2024.08.30 08:18:55 +03'00'
Name:	Silja Häkkinen
Title:	Research Team Leader

Contents

1. Introduction

Micro depletion is an established method in nodal codes for tracking nuclide concentrations in a homogenized reactor geometry. It is mainly adopted for modeling the group constant dependence on historical irradiation conditions. The group constant correction according to depletion history is applied by tracking either nuclides with high importance [1, 2] or nuclides indicating the spectral history [3, 4]. However, the feasibility of micro depletion for detailed inventory calculations remains uninvestigated.

The essence of micro depletion relies on homogenizing and condensing microscopic reaction cross sections for individual nuclides while preserving reaction rates. The homogenization process also averages the initial nuclide content over the node volume. Homogenized microscopic cross sections complemented by decay constants and fission yields are sufficient for describing nuclide transmutation chains in a nodal program, and the burnup problem can be solved with established depletion algorithms.

Nodal program DYN3D applies micro depletion for modeling group constant historical irradiation effects [4] and estimating reactor decay heat power [5]. The decay heat model tracks 1200 distinct nuclides and the local heating power is calculated explicitly based on the decay of nuclides. This report presents a similar methodology implemented in nodal code Ants [6], but the work emphasizes the micro-depletion method for inventory calculations.

This study applies micro depletion for modeling the transmutation of uranium oxide fuel. The work strives to create an equivalent depletion method compared to the Monte Carlo code Serpent [7] which also provides homogenized group constants for Ants [8, 9]. The method is tested for depletion of PWR fuel assembly and the reference is calculated with Serpent while preserving equivalent model parameters for the heterogeneous and homogeneous problem.

This work lays the foundation for calculating full core spent nuclear fuel inventories in the Kraken reactor simulator framework [10]. The objective is to create a general fuel depletion method applicable to multi-physics reactor simulations and back-end fuel cycle studies. In principle, Serpent can conduct these analyses, but it is beyond practical use due to high computational demand. Still, Serpent can validate Ants results, which is also demonstrated in this study.

The rest of this report describes the micro-depletion model and presents a numerical study for analyzing the applicability of the method. Section 2 describes the model, preparation of microscopic cross sections for a nodal diffusion solver, and the test setup for the analysis work. Results of test calculations are presented in Section 3 focusing on the comparison of nuclide inventories and spent fuel properties. Finally, Section 4 summarizes the main findings and addresses the development needs for full-core calculations.

2. Methods

This section presents the micro-depletion model in Ants for fuel depletion and the setup for testing the method. The first three subsections describe the theory and implementation of the model, and the final subsection defines the conducted numerical tests.

2.1 Depletion model in Ants

Similar to Serpent, the fuel depletion problem is modeled by Bateman equations in a matrix exponential form. In each region, the fuel nuclide density is described by a vector $N(t)$ given by the equation

$$N(t) = e^{A(t)}N(0), \tag{2.1}$$

where $A(t)$ is a matrix containing transmutation rates and $N(0)$ is the initial composition. The problem is temporally discretized and the time-dependence is resolved with a predictor-corrector scheme. With the time-discretization, the matrix exponential is solved for each step with Chebyschev Rational Approximation Method (CRAM) [11].

The decay constants and fission yields in the transmutation matrix $A(t)$ are readily available in nuclear data libraries, but the neutron-induced reaction rates have to be calculated separately. Serpent uses the Monte Carlo tracking routine for estimating the reaction rates but the nodal diffusion solver Ants has to rely on the pre-evaluated homogenized microscopic cross sections and homogeneous flux in a multi-group formalism. Hence, the preparation of an equivalent depletion model for a nodal code requires the homogenization and condensation of numerous microscopic cross sections.

For one-to-one compliance with the depletion model in Serpent and micro-depletion method, the set of homogenized reactions has to be created with identical nuclear data libraries. Also, the energy-dependent fission yield tables require dedicated treatment. Equivalent energy-dependent fission yields can be created by separating fission cross sections into multiple cross sections with different yield tables. These can then be used in the nodal diffusion calculation to represent the fission yield distribution. Instead of manually defining all reactions, Serpent can provide a list of all reactions included in a burnup calculation, which can be used to define the required microscopic cross sections for homogenization.

2.2 Homogenization of microscopic cross sections

A recent work revised the microscopic cross section homogenization methodology in Serpent [9], and this report only summarizes the main content. Homogenized microscopic cross sections for reaction x, group g, and nuclide i can be calculated as

$$\sigma^i_{x,g} = \frac{1}{\bar{N}^i \bar{\phi}_g} \frac{1}{V} \int_{E_g}^{E_{g-1}} \int_w \sigma^i_x(E) N^i(r) \phi(r, E)\, dV\, dE. \tag{2.2}$$

Here, V is the volume of the homogenized region, $\bar{\phi}_g$ is the average flux, and $\bar{N}^i$ is the average nuclide density over the whole volume. The user defines the energy group structure and the material occupying subregion w for Serpent, which then estimates the homogenized and condensed microscopic cross section with the Monte Carlo neutron transport.

Microscopic cross sections might need to be homogenized even when the nuclide density $N^i(r)$ is initially zero. In this case, the equation (2.2) is not applicable and the microscopic cross section must be homogenized as

$$\sigma^i_{x,g} = \frac{1}{\bar{\phi}_g} \frac{1}{w} \int_{E_g}^{E_{g-1}} \int_w \sigma^i_x(E) \phi(r, E)\, dV\, dE. \tag{2.3}$$

For example, this form of the equation is used for fresh fuel when the majority of nuclides in the transmutation system are not in the initial composition.

Similar to homogenized macroscopic cross sections, homogenized microscopic cross sections depend on the burnup, instantaneous operational conditions, and historical operational conditions. The distribution and spectrum of neutron flux used in homogenization depend on coolant and fuel properties necessitating the parametrization of homogenized microscopic cross sections. The following subsection describes the model used in this report to represent variations in irradiation conditions.

2.3 Group constant model

This work uses the same model for all homogenized reactor parameters. These include macroscopic and microscopic cross sections, diffusion coefficients, discontinuity factors, and other necessary values. This work refers to all homogenized parameters as group constants for the sake of clarity. In addition, equations use the macroscopic cross section (Σ) for representing all group constants even though they equally apply to other parameters.

The group constant model relies on a polynomial representation of instantaneous operational conditions and plutonium-indicator spectral-history correction method [12] for historical effects. The evaluation of group constants in the nodal calculation starts with interpolating all input parameters at the current burnup from tabulated values. Then, the impact of momentary conditions on group constants is obtained from the polynomial model. Finally, the depletion history spectral effects are corrected with the plutonium-indicator method.

The polynomial model accounts for changes in thermal-hydraulic conditions by estimating the deviation from nominal conditions $\Delta\Sigma(x, \mathrm{bu})$ with a polynomial approximation $P(\Delta x, \mathrm{bu})$. Here, bu indicates the dependence on burnup and x represents state variables e.g. fuel temperature, coolant density, and boron concentration. The polynomial model is constructed by selecting terms for

$$P(\Delta x, \mathrm{bu}) = \sum_m c_m(\mathrm{bu}) \prod_i (\Delta x_i)^{p_{m,i}}, \tag{2.4}$$

where $c_m(\mathrm{bu})$ is the polynomial coefficient of term m, Δx_i is the deviation of a state variable from nominal conditions, and $p_{m,i}$ is the power of the term m and variable i. The coefficients $c_m(\mathrm{bu})$ remain unknown prior to homogenization, and they can be solved with a linear solver in the post-processing phase.

The spectral correction with the plutonium-indicator method relies on the correlation of group constant spectral effects and the local accumulation of ^{239}Pu [12]. In practice, the correction method requires the calculation of an identical set of group constants with a deviated neutron spectrum compared to the nominal history. In the preparatory phase, plutonium coefficients k are evaluated as

$$k = \frac{\Sigma^{\mathrm{offhis}} / \Sigma^{\mathrm{nomhis}} - 1}{\sqrt{N^{\mathrm{offhis}} / N^{\mathrm{nomhis}}} - 1} \tag{2.5}$$

for every homogenized reactor parameter. Here Σ^{nomhis} is a group constant homogenized at nominal conditions and Σ^{offhis} is a group constant evaluated at off-nominal conditions with the deviated irradiation spectrum. Values in the denominator N^{offhis} and N^{nomhis} are ^{239}Pu number densities for both histories respectively.

The actual nodal calculation relies on tracking the concentration of ^{239}Pu with a simplified transmutation chain. Local concentrations and pre-evaluated coefficients $k(x, \mathrm{bu})$ can then be applied for spectral correction. The corrected group constant $\Sigma(x, \mathrm{bu}, N)$ in the nodal calculation is evaluated by

$$\Sigma(x, \mathrm{bu}, N) = \left(1 + \left(\sqrt{N / N^{\mathrm{nomhis}}} - 1\right) k(x, \mathrm{bu})\right) \Sigma^{\mathrm{nomhis}}(x, \mathrm{bu}), \tag{2.6}$$

where N is the actual ^{239}Pu number density, N^{nomhis} is the pre-evaluated nominal history ^{239}Pu number density, and $\Sigma^{\mathrm{nomhis}}(x, \mathrm{bu})$ is the uncorrected nominal history group constant.

2.4 Test calculation setup

The numerical experiment conducted in this report tries to assess if the micro-depletion method can be used to create an equivalent depletion model in a homogeneous system compared to a high-fidelity heterogeneous system. The model is tested in an infinite single-node system which should provide the best agreement between the Ants micro-depletion solver and Serpent burnup solver. The purpose of studying the best-case scenario is to estimate the maximum reachable accuracy of the method when nodal-diffusion-specific approximations are ignored.

The depletion method uses the polynomial model and the plutonium history correction for modeling momentary and past irradiation conditions. The best reachable accuracy could be obtained by using on-the-demand homogenized reactor parameters tailored for each calculation separately. However, this approach would not give any information on the applicability of the group constant model, which is necessary for practical calculations. Hence, this work applies the micro-depletion method with the group constant model for fuel depletion in different operational conditions.

In this test, a PWR fuel assembly is depleted in three different irradiation conditions with constant power up to 60 MWd/kgU burnup. Figure 1 shows the geometry of the fuel model, which follows the 3.4 % enriched fuel specifications without burnable absorbers described in BEAVRS benchmark [13]. One irradiation history is selected equal to the nominal conditions in the group constant generation. The other two histories provide softer and harder neutron spectra, but they are not equal to the group constant off-nominal history. Table 1 shows the selected values for fuel and coolant temperature, coolant density, and boron concentration.

This report selected the following parameters for the PWR fuel group constant model. The state variables were coolant density, boron concentration, and the square root of fuel temperature. The polynomial model contained first- and second-order terms for each variable and a first-order cross term for boron concentration and coolant density. Table 2 shows the conditions for nominal and off-nominal histories and Table 3 shows the momentary branch variations. The depletion was divided into 36 steps with equal spacing compared to the test problem. Group constants were evaluated for nominal points at each step, but branches were evaluated at 16 steps with sparser spacing. All group constants were condensed into two energy groups.

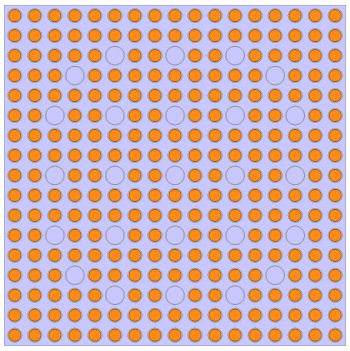

Figure 1. Illustration of a PWR fuel assembly geometry with 3.4 % fuel enrichment from the BEAVRS benchmark.

Table 1. Operational conditions for testing the micro-depletion method for PWR fuel inventory calculations. The power density for all histories is 41.699 W/gU.

History	T_f (K)	T_c (K)	ρ_c (g/cm^3)	C_b (ppm)
Nominal	900	575	0.723	500
Soft	750	555	0.761	450
Hard	1050	595	0.676	550

Table 2. Values of fuel temperature, coolant temperature, coolant density, and boron concentration for nominal and off-nominal depletion calculations in group constant generation.

History	T_f (K)	T_c (K)	ρ_c (g/cm^3)	C_b (ppm)
Nominal	900	575	0.723	500
Off-nominal	1050	587.5	0.692	750

Table 3. Momentary values of fuel temperature, coolant temperature, coolant density, and boron concentration for branch calculations. The branch number eight corresponds to the nominal operational conditions.

Branch	T_f (K)	T_c (K)	ρ_c (g/cm^3)	C_b (ppm)
1	600	550	0.661	0
2	600	550	0.661	500
3	600	550	0.661	1000
4	600	575	0.723	0
5	600	575	0.723	500
6	600	575	0.723	1000
7	900	575	0.723	0
8	900	575	0.723	500
9	900	575	0.723	1000
10	900	600	0.661	0
11	900	600	0.661	500
12	900	600	0.661	1000
13	1200	575	0.723	0
14	1200	600	0.661	0

The depletion problem is solved using Serpent and Ants with equivalent input parameters. Fission yields, decay data, and microscopic cross sections are retrieved from the ENDF/B-VII.1 library. Both codes use 16th-order IPF-type CRAM for solving depletion steps and predictor-corrector method for advancing in time. Each step is further divided into ten substeps and the predictor-corrector scheme relies on linear extrapolation and linear interpolation. ^{135}Xe is the only nuclide evaluated separately in all calculations assuming equilibrium conditions. Parameters for Serpent group constant calculations are identical to reference calculations.

The statistical noise not only affects Serpent results but also Ants results because group constants are evaluated with the Monte Carlo method. To keep the magnitude of stochastic variation in all calculations consistent, all neutron transport calculations have equal neutron populations. Criticality calculations in the group constant generation and depletion calculations have 25 inactive and 100 active cycles with an average of 100 000 neutrons per cycle. The resulting sampling rate is sufficient for providing negligible stochastic noise for most values in interest, but some depletion calculation results are prone to random variation.

Instead of comparing Ants results with a single calculation, the reference is calculated from the mean of ten identical and independent Serpent burnup calculations. The rationale for the selected approach is twofold. First, taking the mean reduces the stochastic noise of the reference compared to Ants results. This enables analyzing the impact of the stochastic variation in Monte-Carlo-based group constants on micro depletion. Second, the approach allows estimating the standard deviation of an equivalent Serpent burnup calculation. The magnitude of stochastic noise in equivalent Serpent results is the smallest expected level of deviation from the reference due to the inherent random error in homogenized input data.

This work analyzes the accuracy of micro depletion by comparing the average number density of Ants-based inventory to the Serpent-based reference at the end of depletion. The analysis is supplemented by the comparison of the infinite multiplication factor and the average scalar flux during irradiation. In addition,

the time behavior is studied by comparing the concentration of a few selected nuclides as a function of burnup. The selected nuclides are either important in reactor physics or back-end fuel studies. Finally, the nuclide inventory at the end of irradiation is used to calculate the activity, decay heat, and photon source rate as a function of cooling time.

3. Results

Comparison of Ants-based micro-depletion results to the reference is divided into the following subsections. The first subsection analyzes the average two-group flux and multiplication factor of the system. The consequent subsections compare the end-of-irradiation nuclide inventory, the transmutation of six distinct nuclides, and the spent fuel properties.

3.1 Multiplication factor and average flux

Figures 2 and 3 show the infinite multiplication factor of the system and the average scalar flux as a function of burnup. The multiplication factor calculated by Ants varies at most 130 pcm from the reference. The largest relative difference of the average scalar flux in the fast group is 0.3 % and in the thermal group 0.7 %. The average thermal flux is slightly underestimated for all depletion histories, and the effect is more pronounced for the soft spectrum.

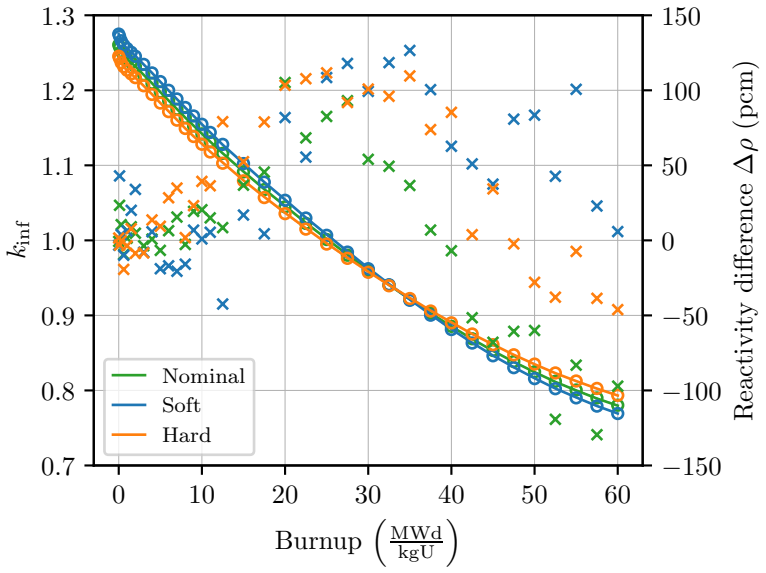

Figure 2. Comparison of neutron multiplication factor between Ants and the reference. Solid lines are Ants results, circles are the reference, and crosses are the relative difference.

3.2 Fuel inventory at the end of depletion

The transmutation model yields 1436 distinct nuclide species for the depleted PWR fuel assembly. The plot in Figure 4a shows the relative difference of the average number density of each nuclide calculated with Ants. Differences are plotted as a function of the reference average number density for easier distinction of abundant and rare species. Respectively, the plot in Figure 4b shows the relative standard deviation associated with a Serpent burnup calculation evaluated with equivalent statistics.

Figure 4a shows that the micro-depletion method calculates a viable solution for all three histories. The majority of species have a relative difference of less than 1 % compared to the reference. Comparing the bulk of points in figures 4a and 4b shows that the difference in Ants results is approximately one order of

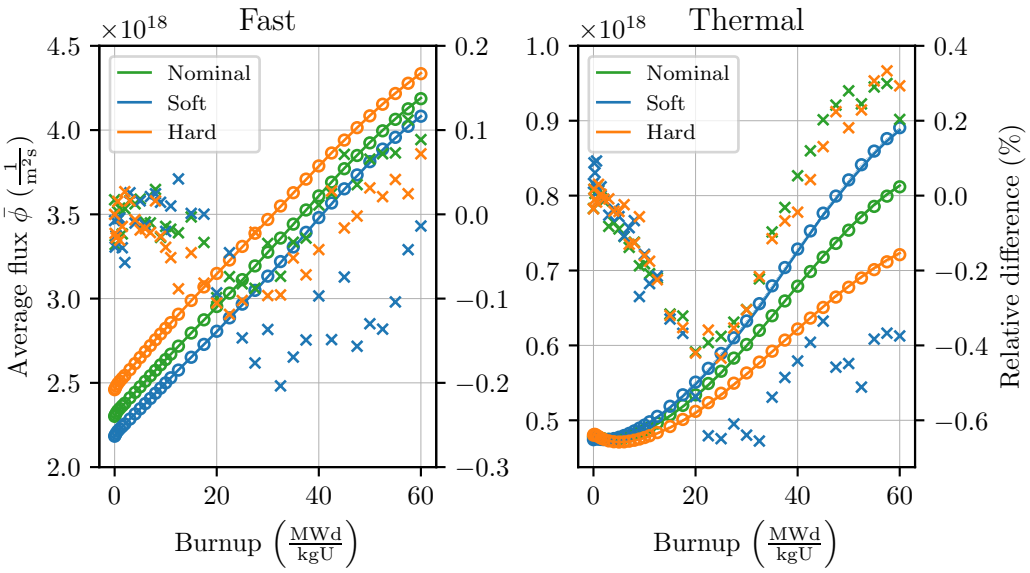

Figure 3. Average fast and thermal flux of the system. Solid lines are Ants results, circles are the reference, and crosses are the relative difference.

magnitude greater than the corresponding stochastic variation. Therefore, the micro-depletion model does not represent the Serpent burnup calculation perfectly, but the agreement between the two models is good.

A significant number of nuclides have deviations from the reference up to tens of percent. However, as Figure 4b shows, Serpent burnup calculations have similar nuclides with high stochastic variation. Therefore, nuclides with high relative differences deviate from the reference likely due to the inherent stochastic error in homogenized microscopic cross sections.

The comparison of Ants and reference inventories reveals additional minor inconsistencies. A total of 33 nuclides are not visualized in Figure 4, because their reference number density is zero. For most nuclides, Ants results agree with the reference, but some have non-zero density up to 10^{-8} $1/m^3$. Furthermore, Ants inventory contains 27 additional nuclides compared to Serpent. These are eighteen different isotopes of Ti, V, Cr, Mn and nine metastable isotopes of In, Sb, Pm, and Eu. The former isotopes have zero density, but the latter have notable concentrations. Nevertheless, the micro-depletion model correctly estimates their stable state number densities.

Table 4 shows the fraction of nuclides calculated with Ants with a lower relative difference than tabulated limits. Similarly, Table 5 shows the standard deviation of an equivalent Serpent burnup calculation. The former table summarizes the reached level of accuracy with the micro-depletion method and the latter table represents the best achievable accuracy expected from the homogenization. Table 5 indicates that for a perfectly equivalent method, approximately 80 % of all nuclides are expected to deviate less than 0.1 % from the reference. However, only 20 to 30 percent of all nuclides calculated with the micro-depletion method reach such a high level of accuracy. Hence, the micro-depletion method does not represent the heterogeneous system perfectly, but the fraction of nuclides deviating less than 1 % from the reference is comparable to a Serpent burnup calculation.

Evaluated nuclide densities are not equally distributed to under and overestimated values as shown in Table 6. At the end of depletion, the nominal and hard depletion histories overestimate the number density for the majority of nuclides. On the contrary, soft history underestimates nuclide concentrations.

The difference between histories is assumed to emerge from the deviation of the average flux. As Figure 3 shows, the average thermal flux for the soft irradiation history is underestimated towards the end of depletion. Lower thermal flux leads to a lower fission rate which reduces the accumulation of fission products leading to underestimated values. The expected outcome for the nominal and hard history is not as clear

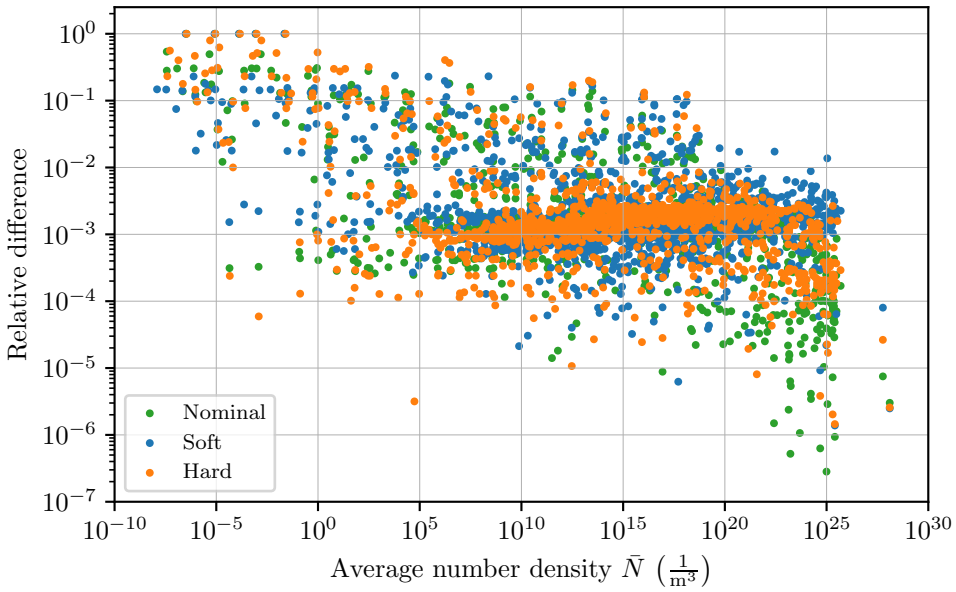

(a) The relative difference of Ants-based results

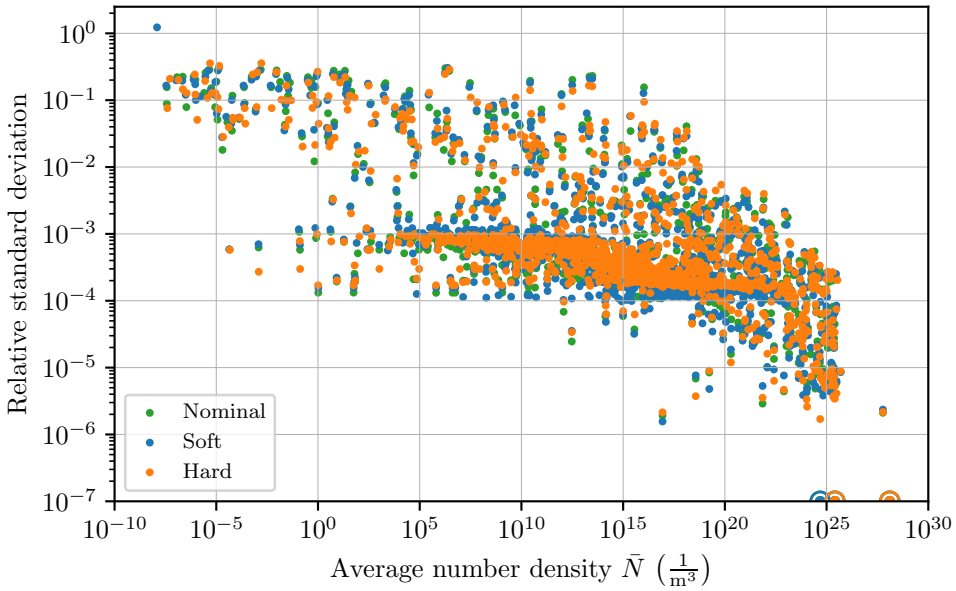

(b) Relative standard deviation of an equivalent Serpent calculation.

Figure 4. The relative difference of Ants results (a) and the standard deviation of an equivalent Serpent burnup calculation (b). Each marker represents results for one nuclide and the color of the marker indicates the depletion history. Circles indicate points that were shifted from outside the plot to the boundary.

Table 4. The cumulative fraction of nuclides with a number density relative difference lower than the tabulated limit. Nuclide number densities are calculated with Ants using the micro-depletion method and compared to the reference calculated from the mean of ten identical Serpent calculations. Each row in the table shows results for each depletion history separately.

Rel. diff.	$< 10^{-4}$	$< 10^{-3}$	$< 10^{-2}$	$< 10^{-1}$	$< 10^{0}$
Nominal	7.1 %	21.7 %	89.1 %	96.4 %	100 %
Soft	1.9 %	30.0 %	86.5 %	96.7 %	100 %
Hard	2.4 %	27.4 %	91.9 %	96.4 %	100 %

Table 5. The cumulative fraction of nuclides from an equivalent Serpent burnup calculation with a relative standard deviation lower than the tabulated limit. The equivalent calculation refers to a burnup calculation with equal statistics compared to calculations used in group constant generation. The standard deviation is estimated from ten repeated Serpent burnup calculations.

Rel. std.	$< 10^{-4}$	$< 10^{-3}$	$< 10^{-2}$	$< 10^{-1}$	$< 10^{0}$
Nominal	9.6 %	78.9 %	89.7 %	96.4 %	100 %
Soft	10.5 %	76.4 %	89.5 %	96.2 %	99.9 %
Hard	9.2 %	79.6 %	88.6 %	97.2 %	100 %

Table 6. The fraction of under and overestimated nuclide number densities calculated with Ants. Values are compared to a reference solution calculated from the mean of ten identical Serpent burnup calculations.

Rel. difference			Nominal		Soft		Hard	
			−	+	−	+	−	+
1	...	10^{-1}	3.6	0.0	1.8	1.5	3.5	0.1
10^{-1}	...	10^{-2}	6.8	0.5	8.7	1.6	3.2	1.3
10^{-2}	...	10^{-3}	7.1	60.3	46.6	9.8	10.9	53.6
10^{-3}	...	10^{-4}	7.4	7.3	22.9	5.3	14.6	10.4
10^{-5}	...	0	3.9	3.1	0.9	1.0	1.1	1.3
		Sum	28.8	71.2	80.8	19.2	33.3	66.7

without detailed analysis. However, both histories have a similar trend in the flux difference and in the distribution of under and overestimated values. These findings suggest that the observed differences in the average flux have a distinguishable impact on the transmutation of nuclides in the depletion system.

3.3 Time behavior

Figure 5 shows the average number density of chosen nuclides as a function of burnup. The first two plots show the time-dependence of main fissile nuclides ^{235}U and ^{239}Pu. The primary mechanism for the depletion of these nuclides is thermal fission and the difference in the thermal flux is reflected in the concentrations of the fissile nuclides. Especially, the soft irradiation history underestimates the fission rate of ^{235}U leading to an overestimated concentration. For other histories, the thermal flux is partially under and overestimated, which compensates for the accumulated error.

Remaining plots in Figure 5 show the accumulation of two minor actinides and two fission products. Ants predicts the average number density of ^{238}Pu and ^{244}Cm accurately demonstrating that the micro-depletion model can solve long transmutation chains. The accumulation of fission products ^{137}Cs and ^{149}Sm and comparison to the reference confirms that fission yields are consistent in the homogenized system.

3.4 Activity, decay heat, and photon emission rate

Figure 6 shows fuel activity, decay heat power, and photon emission rate from short time scales to long time scales after irradiation. All values are derived from the contribution of all decaying nuclides at discharge

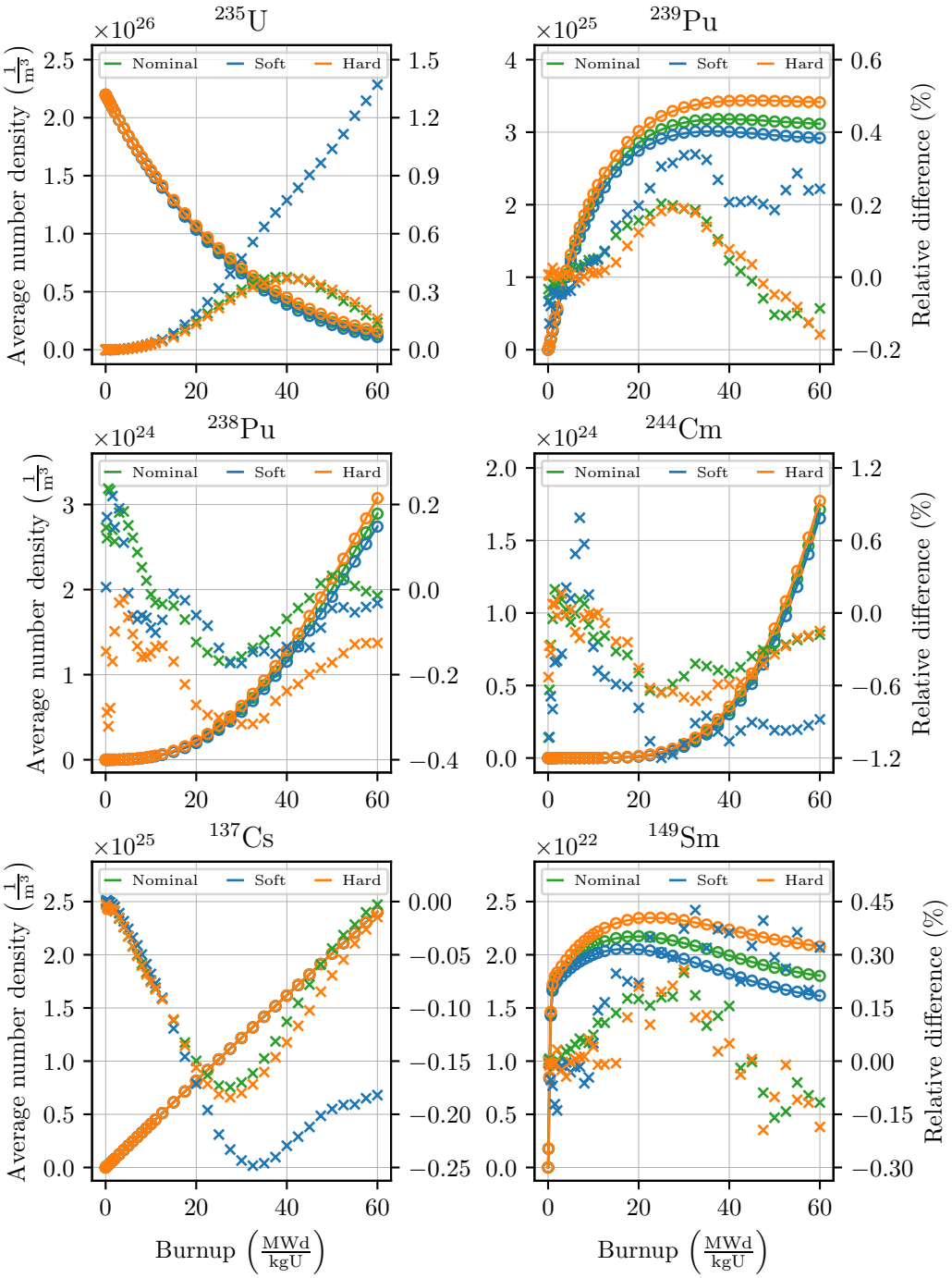

Figure 5. Average number density of six different nuclides as a function of burnup. Solid lines are Ants results, circles are the reference, and crosses are the relative difference.

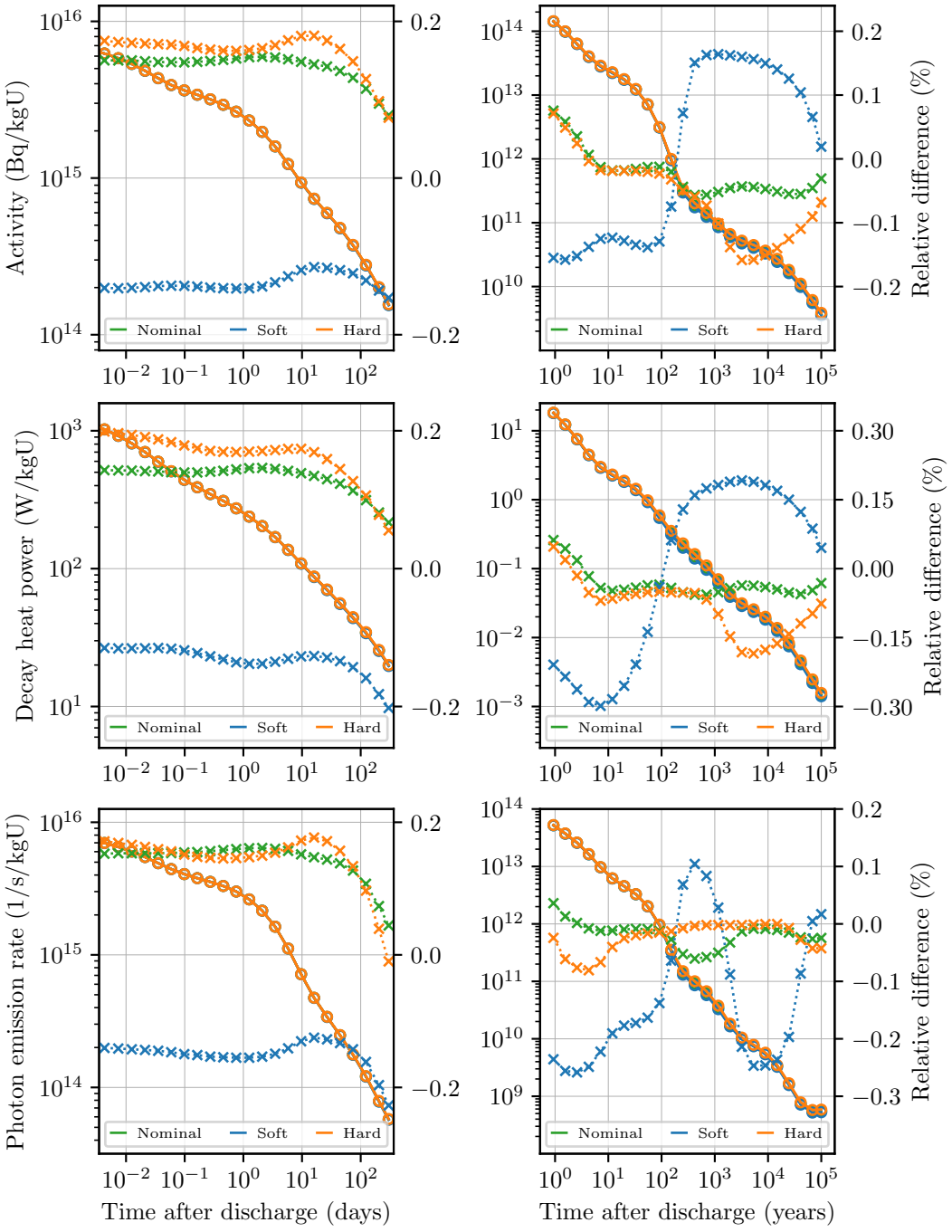

Figure 6. Activity, decay heat power, and photon source rate of fuel as a function of time after the depletion. Solid lines are Ants results, circles are the reference, and crosses are the relative difference

burnup of 60 MWd/kgU. The short timescale on the left-hand side ranges from minutes to a few hundred days and the long timescale on the right-hand side ranges from one year to one hundred thousand years.

The relative difference of micro-depletion based results compared to the reference span from 0.1 to 0.3 %. The deviation is clearly larger than the stochastic variation but equal to or smaller than the difference between the depletion histories. The relative standard deviation of the activity, decay heat, and photon emission rate for an equivalent Serpent burnup calculation is at most 0.03 % which is clearly smaller than the deviation of Ants results. In the short timescale, fuel properties are relatively similar and the relative difference of Ants results is comparable to differences between histories. However, in the long timescales, the soft and hard irradiation history may deviate up to 8 % from the nominal history.

4. Summary and conclusions

This report presented a micro-depletion-based method for fuel inventory calculations applicable to homogenized reactor geometry. The method was successfully used for creating an equivalent uranium oxide fuel transmutation system compared to the continuous energy Monte Carlo transport code Serpent. The model was tested for the depletion of a two-dimensional PWR fuel assembly model with a constant power profile and three different irradiation histories.

For all test calculations, the nuclide inventory agreed well with the Serpent-based reference solution. Out of 1436 distinct species, approximately 90 % of nuclide-wise concentrations deviated less than 1 % from the reference at the end of depletion. The relative difference of fuel activity, decay heat power, and photon emission rate was less than 0.3 % from discharge up to one hundred thousand years. In summary, the micro-depletion method yielded viable fuel inventory estimates accounting for historical operational conditions.

Errors in the micro-depletion method emerge from the group constant model and the inherent stochastic noise. In a thermal system, nuclides formed from high energy threshold reactions are especially subject to high statistical uncertainty in the Monte Carlo neutron transport. Likewise, homogenized microscopic cross sections propagate the stochastic error from the homogenization to the nodal calculation. Consequently, some nuclides may deviate up to tens of percent from the reference solution. However, for most of the relevant nuclides, the limiting factor for the accuracy is the group constant model instead of low sampling rates.

Even though the presented approach yields satisfactory results, practical calculations may require further consideration. First, the transmutation system could be improved and simplified by excluding reactions with low sampling rates. Second, the computational demand of the method has to be assessed in a realistic reactor simulation. The method is clearly faster than Monte Carlo simulations, but it may increase the computational demand of nodal calculations significantly. Finally, the depletion of burnable poisons i.e. gadolinium fuel rods needs further investigation. The depletion of strong absorbers is highly non-linear due to self-shielding, which necessitates either significantly smaller depletion steps or other refined models for accurate calculations [14, 15].

This study enables the micro-depletion development for practical applications in the Kraken reactor simulator framework. The following work involves depleting a 3D core and analyzing the performance of the method. Furthermore, the progress allows feasibility studies of Ants-based fuel inventories for fuel back-end safety analyses.

Acknowledgements

This work has received funding from the NOTCO project under the National Nuclear Safety and Waste Management Research Programme 2023–2028 SAFER2028.

References

[1] Tamer Bahadir, Stenörjan Lindahl, and Scott Palmtag. SIMULATE-4 multigroup nodal code with microscopic depletion model. In *Mathematics and Computation, Supercomputing, Reactor Physics and Nuclear and Biological Applications*, Palais des Papes, Avignon, France, September 2005.

[2] Jinsu Park, Jaerim Jang, Hanjoo Kim, Jiwon Choe, Dongmin Yun, Peng Zhang, Alexey Cherezov, and Deokjung Lee. RAST-K v2—Three-Dimensional Nodal Diffusion Code for Pressurized Water Reactor Core Analysis. *Energies*, 13(23), 2020.

[3] Yurii Bilodid. *Spectral history modeling in the reactor dynamics code DYN3D*. PhD thesis, Technische Universität Dresden, 2014.

[4] Y. Bilodid, D. Kotlyar, E. Shwageraus, E. Fridman, and S. Kliem. Hybrid microscopic depletion model in nodal code DYN3D. *Annals of Nuclear Energy*, 92:397–406, 2016.

[5] Y. Bilodid, E. Fridman, D. Kotlyar, and E. Shwageraus. Explicit decay heat calculation in the nodal diffusion code DYN3D. *Annals of Nuclear Energy*, 121:374–381, 2018.

[6] Ville Sahlberg and Antti Rintala. Development and first results of a new rectangular nodal diffusion solver of Ants. In *Reactor Physics Paving The Way Towards More Efficient Systems, PHYSOR 2018*, pages 3861–3871. American Nuclear Society (ANS), 2018.

[7] Jaakko Leppänen, Maria Pusa, Tuomas Viitanen, Ville Valtavirta, and Toni Kaltiaisenaho. The Serpent Monte Carlo code: Status, development and applications in 2013. *Annals of Nuclear Energy*, 82:142–150, 2015.

[8] Jaakko Leppänen, Maria Pusa, and Emil Fridman. Overview of methodology for spatial homogenization in the Serpent 2 Monte Carlo code. *Annals of Nuclear Energy*, 96:126–136, 2016.

[9] Antti Rintala, Ville Valtavirta, and Jaakko Leppänen. Microscopic cross section calculation methodology in the Serpent 2 Monte Carlo code. *Annals of Nuclear Energy*, 164:108603, 2021.

[10] Jaakko Leppänen, Ville Valtavirta, Antti Rintala, Ville Hovi, Riku Tuominen, Jussi Peltonen, Markus Hirvensalo, Eric Dorval, Unna Lauranto, and Rebekka Komu. Current Status and On-Going Development of VTT's Kraken Core Physics Computational Framework. *Energies*, 15(3), 2022.

[11] Maria Pusa. Higher-Order Chebyshev Rational Approximation Method and Application to Burnup Equations. *Nuclear Science and Engineering*, 182(3):297–318, 2016.

[12] I. Bilodid and S. Mittag. Use of the local Pu-239 concentration as an indicator of burnup spectral history in DYN3D. *Annals of Nuclear Energy*, 37(9):1208–1213, 2010.

[13] Nicholas Horelik, Bryan Herman, Benoit Forget, and Kord Smith. Benchmark for evaluation and validation of reactor simulations (BEAVRS), v1.0.1. In *Proc. Int. Conf. Mathematics and Computational Methods Applied to Nuc. Sci. & Eng*, volume 7, Sun Valley, Idaho, 2013.

[14] Jiwon Choe, Sooyoung Choi, and Deokjung Lee. Analysis of effective gadolinium depletion model. In *Proceedings of the Transactions of the Korean Nuclear Society Spring Meeting*, pages 16–18, Jeju, Korea, May 2018.

[15] Chase Daniel Lawing. *Improved Methodologies for Depletion of Gadolinia Bearing Nuclear Fuel*. PhD thesis, North Carolina State University, 2023.